Transition-metal dispersion on carbon-doped boron nitride nanostructures: Applications for high-capacity hydrogen storage

Ming Chen,[1] Yu-Jun Zhao,[1,2] Ji-Hai Liao,[1] and Xiao-Bao Yang[1,2,*]

[1]*Department of Physics, South China University of Technology, Guangzhou 510640, People's Republic of China*

[2]*Key Laboratory of Clean Energy Materials of Guangdong Higher Education Institute, South China University of Technology, Guangzhou 510640, People's Republic of China*

(Received 22 February 2012; revised manuscript received 7 June 2012; published 31 July 2012)

Using density-functional theory calculations, we investigated the adsorption of transition-metal (TM) atoms (TM = Sc, Ti, V, Cr, Mn, Fe, Co, and Ni) on carbon doped hexagonal boron nitride (BN) sheet and the corresponding cage ($B_{12}N_{12}$). With carbon substitution of nitrogen, Sc, V, Cr, and Mn atoms were energetically favorable to be dispersed on the BN nanostructures without clustering or the formation of TM dimers, due to the strong binding between TM atoms and substrate, which contains the half-filled levels above the valence bands maximum. The carbon doped BN nanostructures with dispersed Sc could store up to five and six H_2, respectively, with the average binding energy of $0.3 \sim 0.4$ eV, indicating the possibility of fabricating hydrogen storage media with high capacity. We also demonstrated that the geometrical effect is important for the hydrogen storage, leading to a modulation of the charge distributions of d levels, which dominates the binding between H_2 and TM atoms.

DOI: 10.1103/PhysRevB.86.045459 PACS number(s): 61.46.−w, 68.43.−h, 73.22.−f

I. INTRODUCTION

Hydrogen has been considered as an ideal energy resource for its high efficiency and environmental friendliness,[1] while the safe and compact storage of hydrogen is the main challenge for the applications. Transition-metal (TM) dispersed nanostructures have been approved to be efficient for the hydrogen storage. For Sc/Ti decorated fullerene,[2] carbon nanotubes,[3] and polymers,[4] the binding energy per H_2 was calculated to be about 0.3 eV and the maximum retrievable H_2 storage density reached $7.6 \sim 9$ wt%, which would be ideal for on-board storage of hydrogen.

It should be noted that the high capacity hydrogen storage is based on the condition that TM atoms coated on the surface will remain isolated. However, TM atoms would form clusters on the surface because the binding energies between TM and substrate were found to be much lower than that of bulk TM structures,[5] leading to a significant liability for the H_2 uptakes. Recently, it was reported that the strong tendency of TM clustering could be efficiently avoided when Ti adsorbed on B-doped, divacancy, divacancy-nitrogen, or oxidized graphene,[6–9] since the charge transfer between dopants (B/N/O) and Ti atoms would significantly increase the binding energies. Embedded in single vacancies in graphene, the binding between TM atoms and the substrate would be strong enough to avoid clustering, due to the TM-C covalent σ bonds.[10] Similarly, TM atoms were found to be isolated for hydrogen storage in metallocarbohedrene systems, such as titanium carbide nanoparticles[11] and boron-based organometallic nanostructures.[12,13] Meanwhile, graphene under a tensile strain of 10%, which could absorb H_2 up to the density of 9.5 wt% when decorated by Ti atoms, was reported to bind strongly with Ti comparable to that between Ti atoms in its bulk.[14]

In most hydrogen storage media based on TM dispersed nanostructures, the high uptake of H_2 is attributed to TM's empty d orbits, which consequently decrease the system stability. Though there is a significant charge transfer from TM atoms to the substrate in metal adsorbed graphene or BN nanostructures, the binding between TM atoms and the substrate is weaker than that between TM atoms, inducing the energetically favored clustering of TM atoms. Herein, we focused on the substrate effect on TM adsorption and explore the possible substrate for a stable TM dispersion. The ideal substrate should contain empty states that will enhance the metal adsorption, and simultaneously, be simple and controllable for synthesis. It was recently demonstrated that carbon atoms or islands can be embedded into boron-nitride (BN) nanostructures by electron-beam-mediated postsynthesis doping.[15] Thus we considered the carbon doped BN sheet as a proper candidate, since the substrate with various doping concentrations and configurations can be easily controlled by electrically charging.[16]

II. METHODS

Our calculations were performed using Vienna *ab initio* simulation package (VASP).[17] We used Vanderbilt ultrasoft pseudopotentials[18] and the exchange-correlation with the generalized gradient approximation given by Perdew and Wang.[19] The plane-wave cutoff energy was set to be 350 eV and the convergence of the force on each atom to be less than 0.01 eV/Å. For the atomic TM adsorption on the BN sheet, a $5 \times 5 \times 1$ supercell was adopted and the Monkhorst-Pack scheme[20] with a **k** mesh of $5 \times 5 \times 1$ was used to sample the Brillouin zone. For the BN cage, the **k** mesh was set to be $1 \times 1 \times 1$. To remove the cell-to-cell interactions, the separation distances were tested from 9 to 20 Å, which varied the total energies less than 0.01 eV. We defined the binding energy of adsorbed atom as $E_b = (E_0 + nE_m - E_d)/n$, where E_d and E_0 are the energies per cell with and without atoms adsorbed and E_m and n are the corresponding energy and number of free adsorbate atoms, respectively. We also defined the formation energy of hydrogen as $E_H = E_{n\mathrm{H_2+complex}} + E_{\mathrm{H_2}} - E_{(n+1)\mathrm{H_2+complex}}$. Here, $E_{n\mathrm{H_2+complex}}$ is the energy per cell with metal atoms and H_2 adsorbed, while $E_{\mathrm{H_2}}$ and n are the corresponding energy and number of H_2, respectively.

III. TRANSITION-METAL DISPERSIONS

We considered the adsorption of an isolated TM atom on the BN sheet (a super cell containing 50 atoms) with a single B or N atom substituted by a C atom [shown in Fig. 1(a)]. Both the substitution at B (C_B-BN) and N (C_N-BN) lattice sites with various charge states can be energetically stabilized, when the electron chemical potential (μ_e) is modulated by charging the structure during irradiation.[15,16] We have calculated the defect formation energies of C_B and C_N in surface and cage, with various charge states in both B-rich and N-rich conditions.

The formation energies of C_B and C_N defect with charge q were calculated as[21]

$$E_f(\mathrm{C_{B/N}},q) = E(\mathrm{C_{B/N}},q) - E(\mathrm{BN}) + \mu_{\mathrm{B/N}} - \mu_{\mathrm{C}} + q(\mu_e + \epsilon_{\mathrm{VBM}}),$$

where $E(C_{B/N},q)$ and E(BN) are the total energies of a supercell containing and without the defect, respectively. The carbon chemical potential μ_C is the same as in graphene, and $\mu_{B/N}$ is B/N chemical potential for the C_B and C_N dopant, respectively. We keep $\mu_B + \mu_N$ as the conservation of the total energy of per BN pair in the BN nanostructure, where $\mu_B(\mu_N)$ is the same as in the bulk boron (N_2 molecule) for the B-rich (N-rich) environment. μ_e is the electron chemical potential, with respect to the valence band maximum ε_{VBM}. In general, a potential alignment (ΔV) to the VBM, and an image charge correction [$\Delta E_{el}(q)$] to the total energy of $E(C_{B/N},q)$ are required due to the interaction between the defect and its periodic images, especially for the simulation of defects in extremely low concentrations. A general and efficient scheme, however, is still not available in spite of numerous attempts.[22–24] Meanwhile, in this work, the defects are intended to afford sufficient adsorption sites for the TM for hydrogen storage. Therefore a rather high concentration of defects is expected, and thus the corrections are less important than that for the defects providing carriers in semiconductors. The formation energies presented in Fig. 1(b) were calculated without corrections to the image charge correction and potential alignment. Nevertheless, we investigated the influence of the corresponding corrections to the stability of neutral $C_{N/B}$ on BN sheet/cage here, by employing a simple and reliable correction scheme reported recently.[24] The results showed that the corrections at both the sheet (with the $5 \times 5 \times 1$ supercell) and the cage were within 0.4 eV, with $\Delta E_{el}(q)$ around 0.4 eV and ΔV within 0.01 eV, which would increase the formation energies of charged defects. Thus, the neutral state of C_N dopant should be stable in larger range of electron chemical potential, which would be proper for the further TM adsorption.

As shown in Fig. 1(b), the neutral states of C_N-BN sheets are stable in the N-rich environment when μ_e is lower than 1.3 eV with respect to the valence band maximum (VBM), while the 1− charge states are preferred for $\mu_e > 1.3$ eV. The neutral states and 1+ charge states of C_B-BN are stable for $\mu_e > 2.7$ eV and $\mu_e < 2.7$ eV, respectively. In the neutral state with N-rich condition, it is energetically favorable for more B than N atoms to be substituted with C, which is in agreement with the results reported in Ref. 16. In the B-rich environment, substitution of N atoms with C is more stable and the neutral state is preferred for $\mu_e < 1.3$ eV. Similarly, the neutral state of C_N-BN cage is stable in the B-rich environment with $\mu_e < 2.1$ eV.

It is found that a Sc atom prefers to adsorb on the hollow site of the hexagon with substitutional C atom [shown in Fig. 1(a)], and the adsorption is much more stable for Sc on the C_N-BN sheet than that on the C_B-BN, with the binding energies of 3.02 and 1.55 eV, respectively. With C substitution of B or N, it will either introduce an extra electron or deplete a valence electron, inducing C p_z level dominated gap states, which are half-filled at neutral charge state. As shown in Fig. 1(c), the Fermi level of C_B-BN sheet is near the conduction band maximum (CBM), while it shifts to VBM for the C_N-BN sheet. When acceptor-like levels exist in the ligand, the charge transfers would lead to a stronger TM binding (verified by the calculated binding energies) on the C_N-BN sheet than the C_B-BN sheet, in a good agreement with a recent report.[25] Thus we focus on the TM adsorption on the C_N-BN sheet.

In general, metal atoms tend to form clusters on the surface of nanostructures if the binding energies are much lower than that of their bulks.[26] For example, the binding energies for

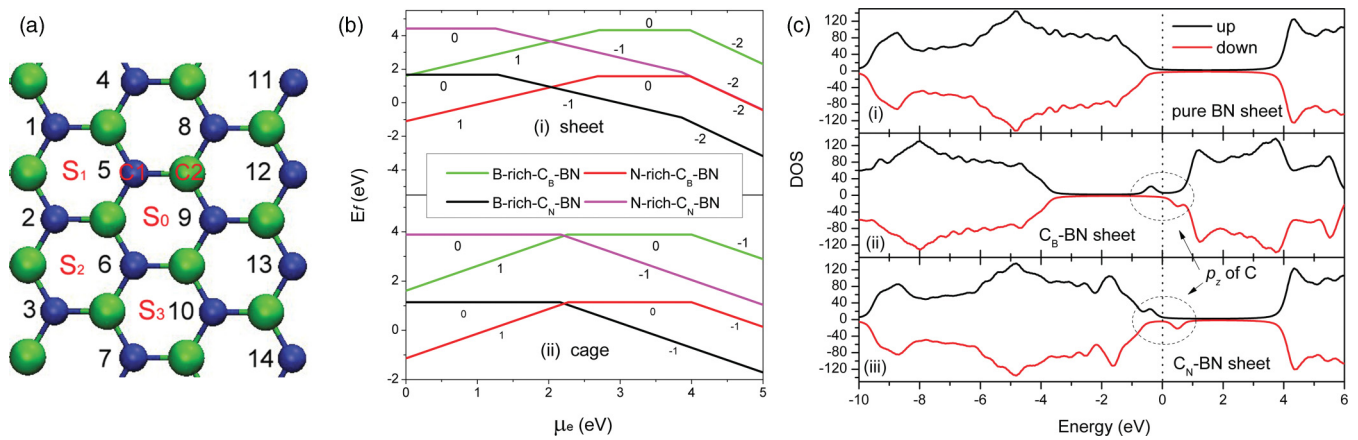

FIG. 1. (Color online) (a) The C-doped BN sheet. Green and blue balls represent boron and nitrogen atoms, respectively. C1 and C2 represent the positions substituted by carbon, while S0, S1, S2, and S3 represent the possible adsorption sites of TMs. $1 \sim 14$ are marked to show the possible substitution of N atoms by carbon. (b) Formation energies of substitutional defects in different charge states as functions of electron chemical potential. (c) Density of states of (i) pure, (ii) C_B-BN sheet, and (iii) C_N-BN sheet. The Fermi level is set to be zero.

TABLE I. The binding energies of one (E_{b1}) and two (E_{b2}) TMs on the C_N-BN sheet in eV/TM, along with the cohesive energies of bulk TMs from calculations (E_{coh}^{cal}) and experiments (E_{coh}^{exp}).[27]

Element	Sc	Ti	V	Cr	Mn	Fe	Co	Ni
E_{b1} (eV)	3.02	3.03	2.73	2.16	2.04	2.86	2.61	2.89
E_{b2} (eV)	2.68	2.90	2.36	1.84	1.46	2.85	2.65	2.89
E_{coh}^{cal} (eV)	3.99	5.08	5.03	3.36	3.02	5.19	4.99	4.94
E_{coh}^{exp} (eV)	3.90	4.85	5.31	4.10	2.92	4.28	4.39	4.44

Sc on graphene and BN sheet were found to be 1.34 and 0.26 eV, respectively, while that in bulk Sc was calculated to be 3.99 eV. When one more Sc atom is added, the binding energies will increase markedly as a dimer forms (to 2.12 and 1.11 eV/Sc for graphene and BN sheet, respectively). Thus there is a strong tendency of clustering for Sc on these two sheets. Table I shows the binding energies of single TMs and TM dimers on C_N-BN sheet, as well as the cohesive energies of bulk TMs from calculations (E_{coh}^{cal}) and experiments (E_{coh}^{exp}) for comparisons. Note that the difference between the binding energy of Sc on ideal graphene (BN sheet) and that in its bulk is 2.65 (3.73) eV/Sc, while this difference is reduced to around 1 eV for Sc on C_N-BN sheet. Furthermore, the clustering tendency of TM atoms could be avoided if the dimer adsorption was not stable compared to the isolated adsorption, even if the binding energies were still lower than those in their bulk structures.[27]

We considered all possible dimer configurations and defined the clustering energy ($E_{clustering}$) as the binding energy difference between the dimer (E_{b2}) and dispersed adsorption of TM atoms (E_{b1}): $E_{clustering} = E_{b2} - E_{b1}$. Here, E_{b2} is the binding energy of TM (in eV/TM) corresponding to the dimer with the lowest total energy, and positive (negative) $E_{clustering}$ stands for TM atoms tend to be clustering(dispersed). Figure 2(a) shows the clustering energy for various TM atoms. There is still clustering tendency for Co as the clustering energy keeps positive. For Ti, Fe, and Ni, the distributions are expected to be rather random since the clustering energies are less than 0.15 eV. The distribution of Sc, V, Cr, and Mn will be clearly dispersive as the isolated TM atoms are favored by more than 0.3 eV/atom. Figures 2(b) and 2(c) show the atomic processes of Sc adatom and dimer on C_N-BN sheet from the first-principles molecular dynamic simulations with the temperature at 300 K and the time step of 0.5 fs. We used a BN sheet with one N atom substituted by C, and the Sc adatom was initially placed on the hollow site of BN hexagon, with the C-Sc distance of 4.36 Å. It was found that Sc atom gradually diffused towards the C defect and was finally trapped around with the C-Sc distance around 2.1 Å. For a Sc dimer, we used a BN sheet with two N atoms substituted by C and set the initial position of 3.0 Å above the sheet with the Sc-Sc distance of 2.66 Å (the optimized distance for a free Sc dimer). Approaching to the sheet, the Sc-Sc dimer dissociated to Sc adatoms and was gradually trapped around the carbon dopants, with the Sc-Sc distance of more than 3.5 Å.

When Sc is adsorbed on the C_N-BN sheet, one s electron transfers to the substrate and fills in the C p_z orbit. The magnetic moment of the system is $2.0\mu_B$, attributed to the other unpaired s electron and one d electron. The charge transfer enhances the Coulomb interaction between the metal atoms and BN sheet, and thus stabilizes the adsorption. For the dimer adsorption, the bonding between TM atoms is weakened due to the charge trapping by the substrate. Meanwhile, the charge transfer raises the strong electrostatic repulsion between TM atoms, which will decrease the dimer stability and make the dispersion energetically favorable.

According to the defect formation energies, the C_N-BN sheet is stable under the B-rich condition. By modulating the chemical potential of B, N, C atoms, the concentration of C_N dopants will be controlled. We also considered the possible configurations of multiple C_N dopant. With two C_N dopants at the positions of (1, 2), (1, 8), (1, 3), and (1, 7) [shown in Fig. 1(a)], the formation energies of neutral state per C_N dopant in the N-rich environment were calculated to be 9.63, 9.68, 9.70, and 9.65 eV, respectively. For three C_N dopants, the formation energies of neutral state per C_N dopant were 9.67, 9.67, 9.67, 9.65, and 9.67 eV, for the substituted positions of (1, 5, 10), (1, 3, 9), (1, 2, 6), (1, 3, 5), and (1, 2, 5), respectively. Thus the stability of C_N dopants is almost independent of the distance of C_N dopants and the substituted configurations, with the differences in the order of 10 meV. As the concentration increases, C_N dopants should be distributed randomly without clustering under room temperature, which would trap the TM adatoms during their diffusion and make them dispersed.

IV. HYDROGEN STORAGE

According to the calculated binding energies, the adsorbed Sc, V, Cr, and Mn would be dispersed on the C_N-BN sheet and might be further applied for hydrogen storage. Here, we focused on Sc, the lightest element, to achieve a high storage density of H_2. For H_2 adsorption on TM dispersed C doped BN sheet, we used a $3 \times 3 \times 1$ supercell with two N atoms substitution of C. As shown in the inset of Fig. 3, the consecutive adsorption energy of H_2 ranges from 0.18 to 0.68 eV, as the number of H_2 adsorbed increases from one to four. Each Sc atom can absorb up to 5 H_2, i.e. 6.1 wt% with the adsorption energy of 0.06 eV for the fifth H_2. We have also confirmed that Sc dispersion is energetically favored on C_N-BN cage, with Sc on the top site above the C atom. On the C_N-BN cage, the adsorption energy of H_2 is 0.16 eV for the first H_2 and 1.05 eV for the fourth H_2. Each Sc atom can absorb up 6 H_2 with the adsorption energy of 0.15 eV for the sixth H_2, corresponding to the hydrogen density of 5.9 wt%.

The adsorption number f of H_2 on per Sc atom under thermal equilibrium with its ambient was calculated as[4]

$$f = kT\frac{\partial \ln Z}{\partial \mu} = \frac{\sum_{l=0} l g_l e^{l(\mu-\varepsilon_l)/kT}}{\sum_{l=0} g_l e^{l(\mu-\varepsilon_l)/kT}},$$

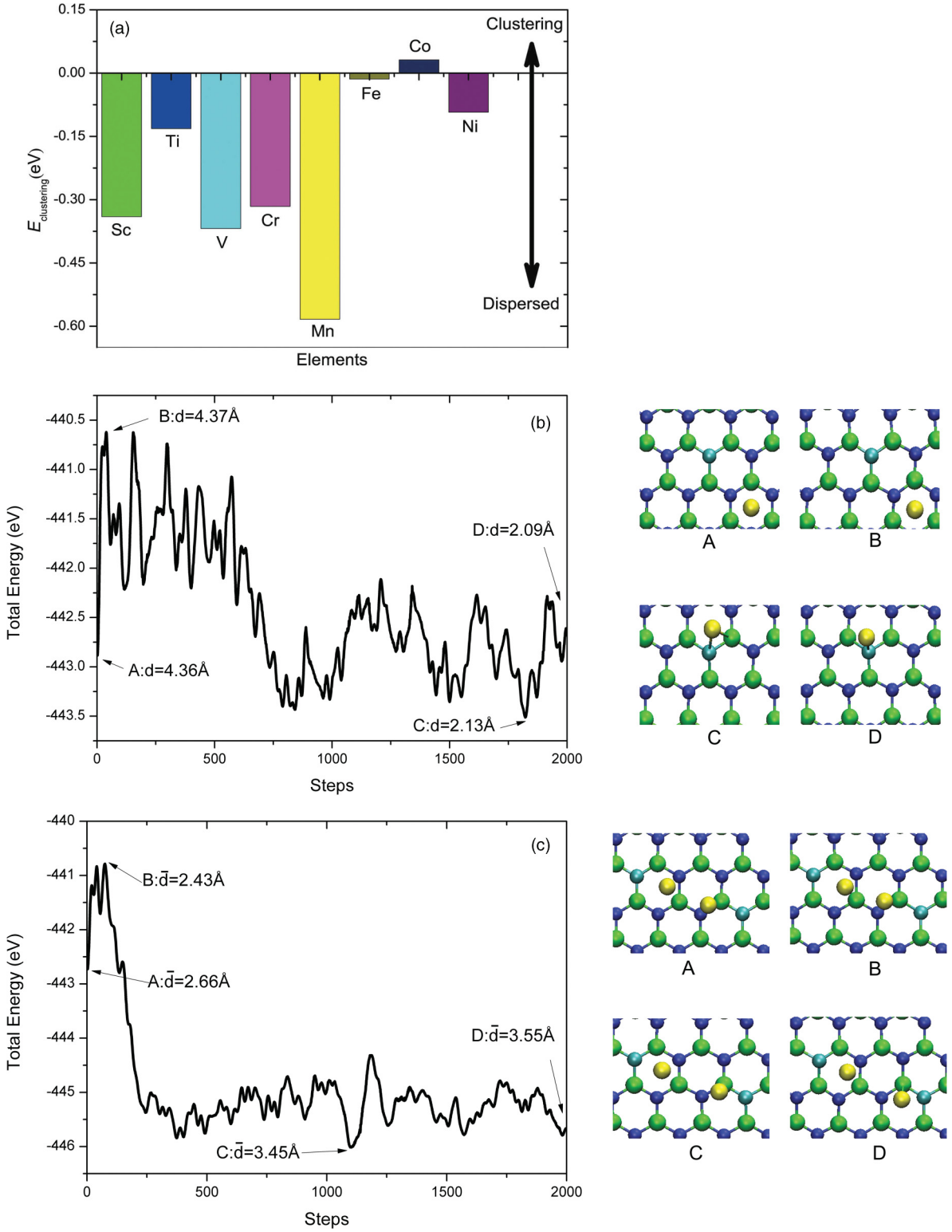

FIG. 2. (Color online) (a) Clustering energy ($E_{clustering}$) on C_N-BN sheet. Negative $E_{clustering}$ indicates that TMs prefer to be dispersed. (b) Sc adatom and (c) Sc dimer diffusion on C_N-BN sheet from the first-principles molecular dynamic simulations.

where Z is the grand partition function and k is the Boltzmann constant. μ is the chemical potential of H_2 in the gas phase at given pressure p and temperature T, which can be obtained under the approximation of an ideal gas.[28] We set the degeneracy factor g_l to be 1, since it was turned out to give a minor correction to the result.[4] Figure 3 shows the uptakes of H_2 as a function of temperature with various pressures. There are two platforms for the release of H_2. For Sc dispersed C_N-BN sheet under the atmospheric pressure, the first H_2 will be released at about 100 K and the other four H_2 will desorb

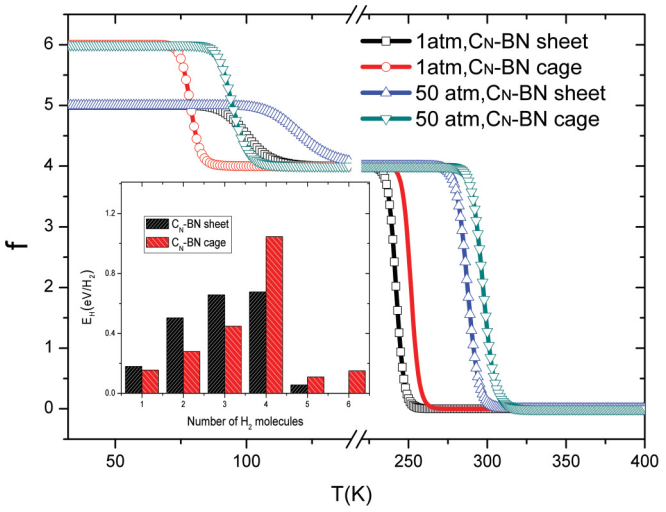

FIG. 3. (Color online) Number of adsorbed H_2 per Sc atom under thermal equilibrium as a function of temperature at 1 atm and 50 atm. (Inset) Consecutive adsorption energies of H_2 per Sc on the C_N-BN sheet and cage as a function of the number of H_2.

at about 250 K. Each Sc on the C_N-BN cage can absorb up 6 H_2 when $T < 75$ K at $p = 1$ atm and 4 H_2 when T ranges between 75 and 250 K. When the pressure increases to 50 atm., the release temperature will be shifted to around 300 K, which is suitable for the on-board storage of hydrogen. Note that the number of usable H_2 per Sc atom is four around ambient temperature and low pressure for both the C_N-BN sheet and cage, corresponding to the density of 4.9 wt% and 4.1 wt%, respectively.

In the following, we analyze the electronic properties of the system to study the binding between H_2 and the TM dispersed substrate. Figure 4 shows the Sc's PDOS on the C_N-BN sheet with various H_2 adsorbed. Before the uptakes of H_2, there is only one d electron of Sc at $d_{x^2-y^2}$ level, with many empty d levels near the Fermi level. With the adsorption of one or two H_2, Sc's d levels are gradually filled due to the charge transfer from H_2 molecules. As the number of H_2 increases, the gap between the filled and empty levels appears. The abrupt increase of gap for the system with adsorption of five H_2 implies a saturation of H_2 uptakes, in line with the adsorption energy platform of H_2 (shown in the inset of Fig. 3). There are unfilled d levels of Sc though; it is difficult for further uptakes of H_2 since the geometrical blocking induced by preadsorbed H_2 will prevent extra H_2 adsorption.

In a previous report,[2] the maximum uptake of H_2 for a TM atom will satisfy the 18-electron rule and the d levels are gradually saturated by H_2. Thus the maximum number of adsorbed H_2 is expected to increase if we decrease the number of electrons contributed by the substrate. For the C_N-BN cage, it is energetically favored for Sc on the top site above the C atom and the substrate only provides one electron. The maximum number of adsorbed H_2 on each Sc atom should be seven according to the 18-electron rule. However, it is found to be six for the Sc dispersed C_N-BN cage. Figure 5 shows the PDOS of Sc dispersed C_N-BN cage with various H_2 adsorption, as well as the charge distributions of the highest-occupied molecular orbitals (HOMOs) and lowest-unoccupied molecular orbitals (LUMOs). Before the uptake of H_2, the d_{xy} level is half-filled and the charge distribution of HOMO displays the same shape as the d_{xy} level, as shown in Fig. 5(b). When there are four H_2 adsorbed, the d_{xy} level is full-filled due to the charge transfer from H_2 as both verified by the PDOS analysis and the charge distribution of HOMO. The bonding between H_2 and Sc is dominated by the d_{xy} level, which is in agreement with previous study of hydrogen adsorption on TM dispersed carbon nanostructure.[29,30] The LUMO is the d_{z^2} level and there are more H_2 that can be adsorbed. With six H_2 adsorbed, HOMO still corresponds to the d_{xy} level, while LUMO corresponds to the unfilled d_{yz} level, which can adsorb no extra H_2.

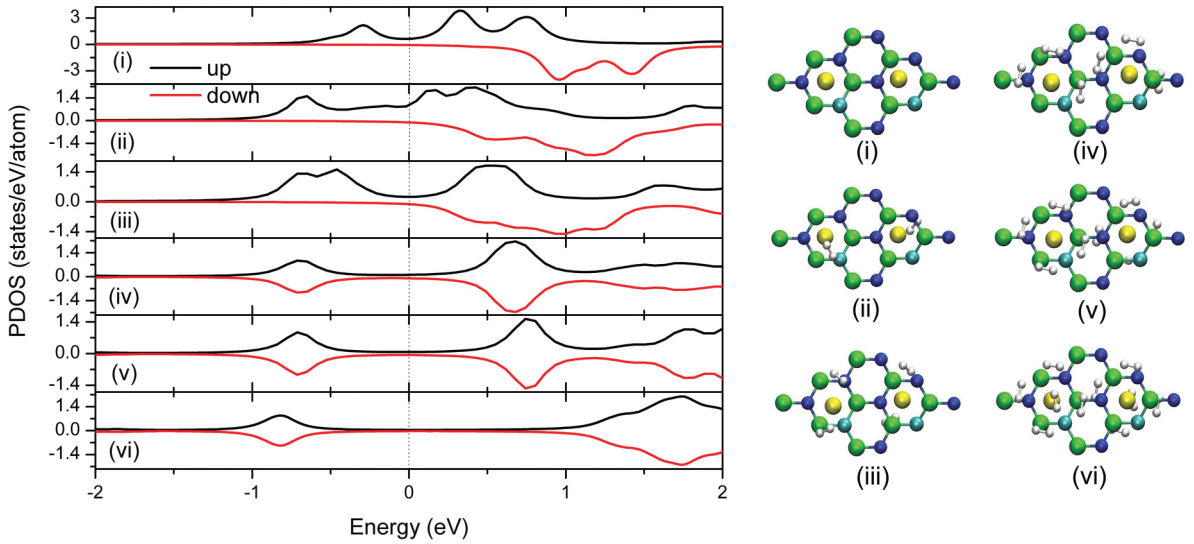

FIG. 4. (Color online) The PDOS (i ∼ vi) of the dispersed Sc with the adsorption of 0 ∼ 5 H_2 on the C_N-BN sheet and corresponding top views of the atomic configurations. (Sc: yellow ball; B: green ball; N: blue ball; C: light blue ball; H: silver ball). The Fermi level is set to be zero.

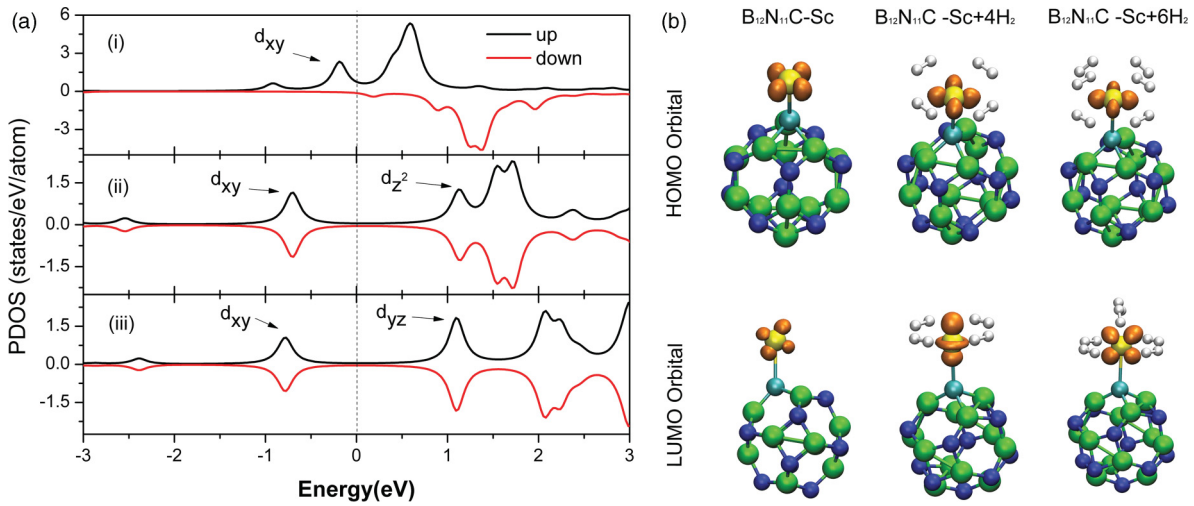

FIG. 5. (Color online) (a) The PDOS of the dispersed Sc corresponding to adsorption of 0, 4, and 6 H_2 (i $\sim$ iii) on the C_N-BN cage. (b) The charge distributions of d levels with various H_2 adsorptions, with the isovalue of 0.15 e/Å^3. The Fermi level is set to be zero.

In our calculations, we found that the binding between H_2 and the d_{xy} level is strong and the four H_2 at a dispersed Sc atom stabilizes the d_{xy} level according to the crystal field theory. Even at a low chemical potential of H, the dispersed configurations of Sc-$n$$H_2$ ($n < 4$) is energetically unstable with respective to that of Sc-4H_2 coupled with other Sc without H_2. Thus, there is a platform of four for the uptakes of H_2 and the adsorption number of H_2 will decrease from four to zero per Sc as the temperature increases (shown in Fig. 3). Besides, the Sc dispersed C_N-BN sheet and cage are stable when there are five and six H_2 on each Sc atom respectively, which corresponds to another platform for the uptakes of H_2 as a function of the temperature. In addition, no extra H_2 could be adsorbed though there are unfilled d levels around Fermi level, implying that the geometrical blocking has a great effect on the maximum number of H_2 adsorption, as well as the 18-electron rule.

V. CONCLUSIONS

In conclusion, we demonstrated that TMs (Sc, V, Cr, and Mn) were energetically favorable to be dispersed on the C_N-BN sheet and cage, which could uptake H_2 with the density of about 6 wt%. There would be four usable H_2 per Sc atom for both the C_N-BN sheet and cage (i.e., 4.9 wt% and 4.1 wt%, respectively) around ambient temperature and low pressure, indicating the potential applications for the on-board storage of hydrogen. With the acceptor-like levels, the carbon dopants served as the potential wells for trapping TM atoms and avoiding the clustering of TM effectively, as was verified by the molecular dynamics simulations. Besides the 18-electron rule, the geometrical blocking would have a great effect on the maximum number of H_2 adsorption. The uptakes of H_2 should be improved if all the empty d levels are made available by removing the geometrical blocking.

ACKNOWLEDGMENTS

This work was supported by MOST under project 2010CB631302, NSFC (Grant No. 11104080), the Fundamental Research Funds for the Central Universities (Grant No. 2011ZM0090), and The Project Supported by Guangdong Natural Science Foundation (S2011040005430).

*scxbyang@scut.edu.cn

[1] L. Schlapbach and A. Zuttel, Nature (London) **414**, 353 (2001).
[2] Y. F. Zhao, Y. H. Kim, A. C. Dillon, M. J. Heben, and S. B. Zhang, Phys. Rev. Lett. **94**, 155504 (2005).
[3] T. Yildirim and S. Ciraci, Phys. Rev. Lett. **94**, 175501 (2005).
[4] H. Lee, W. I. Choi, and J. Ihm, Phys. Rev. Lett. **97**, 056104 (2006).
[5] Q. Sun, Q. Wang, P. Jena, and Y. Kawazoe, J. Am. Chem. Soc. **127**, 14582 (2005).
[6] K. Gyubong, J. Seung-Hoon, and P. Noejung, Appl. Phys. Lett. **92**, 013106 (2008).
[7] L. Wang, K. Lee, Y. Y. Sun, M. Lucking, Z. F. Chen, J. J. Zhao, and S. B. B. Zhang, Acs Nano **3**, 2995 (2009).
[8] W. I. Choi, S. H. Jhi, K. Kim, and Y. H. Kim, Phys. Rev. B **81**,085441 (2010).
[9] S. B. Chu, L. B. Hu, X. R. Hu, M. K. Yang, and J. B. Deng, Int. J. Hydrog. Energy **36**, 12324 (2011).
[10] A. V. Krasheninnikov, P. O. Lehtinen, A. S. Foster, P. Pyykkö, and R. M. Nieminen, Phys. Rev. Lett. **102**, 126807 (2009).
[11] Y. F. Zhao, A. C. Dillon, K. Yong-Hyun, M. J. Heben, and S. B. Zhang, Chem. Phys. Lett. **425**, 273 (2006).
[12] S. Meng, E. Kaxiras, and Z. Y. Zhang, Nano Lett. **7**, 663 (2007)
[13] Y. F. Zhao, M. T. Lusk, A. C. Dillon, M. J. Heben, and S. B. Zhang, Nano Lett. **8**, 157 (2008).
[14] M. A. Zhou, Y. H. Lu, C. Zhang, and Y. P. Feng, Appl. Phys. Lett. **97**, 103109 (2010).

[15]O. L. Krivanek, M. F. Chisholm, V. Nicolosi, T. J. Pennycook, G. J. Corbin, N. Dellby, M. F. Murfitt, C. S. Own, Z. S. Szilagyi, M. P. Oxley, S. T. Pantelides, and S. J. Pennycook, Nature (London) **464**, 571 (2010).

[16]N. Berseneva, A. V. Krasheninnikov, and R. M. Nieminen, Phys. Rev. Lett. **107**, 035501 (2011).

[17]G. Kresse and J. Furthmuller, Phys. Rev. B **54**, 11169 (1996).

[18]D. Vanderbilt, Phys. Rev. B **41**, 7892 (1990).

[19]J. P. Perdew, J. A. Chevary, S. H. Vosko, K. A. Jackson, M. R. Pederson, D. J. Singh, and C. Fiolhais, Phys. Rev. B **46**, 6671 (1992).

[20]H. J. Monkhorst and J. D. Pack, Phys. Rev. B **13**, 5188 (1976).

[21]S. B. Zhang and J. E. Northrup, Phys. Rev. Lett. **67**, 2339 (1991).

[22]C. Persson, Y.-J. Zhao, S. Lany, and A. Zunger, Phys. Rev. B **72**, 035211 (2005).

[23]C. Freysoldt, J. Neugebauer, and C. G. Van de Walle, Phys. Rev. Lett. **102**, 016402 (2009)

[24]S. E. Taylor and F. Bruneval, Phys. Rev. B **84**, 075155 (2011)

[25]G. Kim, S.-H. Jhi, N. Park, S. G. Louie, and M. L. Cohen, Phys. Rev. B **78**, 085408 (2008).

[26]X. Yang, R. Q. Zhang, and J. Ni, Phys. Rev. B **79**, 075431 (2009).

[27]M. Chen, X. B. Yang, J. Cui, J. J. Tang, L. Y. Gan, M. Zhu, and Y. J. Zhao, Int. J. Hydrog. Energy **37**, 309 (2012).

[28]X. Yang and J. Ni, Phys. Rev. B **74**, 195437 (2006).

[29]B. Kiran, A. K. Kandalam, and P. Jena, J. Chem. Phys. **124**, 224703 (2006).

[30]H. Lee, W. I. Choi, M. C. Nguyen, M.-H. Cha, E. Moon, and J. Ihm, Phys. Rev. B **76**, 195110 (2007).